



Simple Approach to Accurately Predict Pharmacokinetics of Therapeutic Monoclonal Antibodies after Subcutaneous Injection in Humans

Kenta Haraya¹ · Tatsuhiko Tachibana¹

Published online: 11 August 2020
© Springer Nature Switzerland AG 2020

Abstract

Background and objective The subcutaneous injection of therapeutic monoclonal antibodies is increasingly used in the treatment of several diseases because of its convenience. Thus, a simple and accurate method of predicting the pharmacokinetics of monoclonal antibodies after a subcutaneous injection in humans would be a valuable tool for preclinical/clinical development. In this study, we investigated whether the pharmacokinetics of monoclonal antibodies after a subcutaneous injection in humans can be predicted using only pharmacokinetic data after a subcutaneous injection in cynomolgus monkeys.

Methods First, we compared the accuracy of three approaches to predict the apparent clearance (CL/F) and apparent volume of distribution (V_d/F) for 15 monoclonal antibodies in humans (1) allometric scaling from cynomolgus monkeys; (2) geometric mean of reported values in humans; (3) estimation from a regression line based on CL/F in humans [only V_d/F]. Then, using the predicted CL/F and V_d/F , and the geometric mean of reported absorption rate constant of mAbs the plasma concentration–time profiles of 13 monoclonal antibodies after subcutaneous injections in humans were simulated.

Results In a comparison of approaches, the first approach showed the best prediction accuracy for CL/F with an exponent of 0.9 (100% and 73% prediction accuracy within 2- and 1.5-fold of the observed value), and the third approach was the best for V_d/F (100% prediction accuracy within 1.5-fold of the observed value). Next, using the first approach for CL/F and the third approach for V_d/F , we accurately predicted the plasma concentration–time profiles of 13 monoclonal antibodies after subcutaneous injections in humans.

Conclusion This simple approach can be applied in preclinical and clinical settings to predict the pharmacokinetics of monoclonal antibodies after subcutaneous injections in humans. Further, this approach requires only CL/F after a subcutaneous injection in cynomolgus monkeys, contributing to animal welfare and reducing costs.

Key Points

Human pharmacokinetics of monoclonal antibodies after a subcutaneous injection was accurately predicted from only three parameters based on the pharmacokinetic data after a subcutaneous injection in cynomolgus monkeys.

Our simple approach does not require the pharmacokinetic data after an intravenous injection in animals, contributing to animal welfare, and reducing costs.

1 Introduction

Therapeutic monoclonal antibodies (mAbs) have become an important therapeutic option for several diseases including cancer, autoimmune diseases, and infectious diseases [1, 2]. The advantages of mAbs over other therapeutic formats (small-molecule drugs, peptide drugs, and other protein drugs) are high specificity, strong binding affinity against the target antigen, and superior pharmacokinetic properties (in particular the long half-life, small clearance [CL], and high subcutaneous bioavailability). Although mAbs cannot be orally administered owing to their instability in the stomach and intestine and their poor penetration of the intestinal epithelial barrier, there are several other options for delivering mAbs into systemic circulation such as intravenous (IV), subcutaneous (SC), and intramuscular injection [3].

✉ Kenta Haraya
haraya.kenta@chugai-pharm.co.jp

¹ Chugai Pharmaceuticals Co., Ltd., 1-135 Komakado, Gotemba, Shizuoka 412-8513, Japan

Subcutaneous injection is an effective administration route, especially for patients with chronic diseases. Self-injection is convenient for both hospitals and patients because a hospital visit is not needed. Even if administered at a hospital, self-injection does not require a hospital bed, making long-term stays unnecessary and allowing hospitals to better manage bed occupancy. Because of these advantages, SC injection has been recently applied in clinical settings for a variety of mAbs [4]. Furthermore, several novel technologies, such as “recycling antibody” [5], “sweeping antibody” [6–8], and application of hyaluronidase [9], have been developed to reduce the required dosage or increase injection volume [10]. These technologies can further increase the number of SC formulations in development.

In the preclinical development of mAbs, cynomolgus monkeys are frequently used to evaluate pharmacokinetics, pharmacodynamics, and safety owing to the high homology of target antigens and comparable FcRn-binding properties with humans [11]. Cynomolgus monkeys are also reported to be good for predicting the pharmacokinetics of mAbs in humans [12, 13]. In both species, the linear pharmacokinetic profile of mAbs after IV and SC injections are captured well by six parameters: CL, inter-compartmental CL (Q), volume of distribution in the central compartment (V_c), volume of distribution in the peripheral compartment (V_p), absorption rate constant (k_a), and bioavailability (F) [14–17]. Thus, we previously established an approach for predicting all six parameters, including the plasma concentration–time profile after IV and SC injections in humans [12]. In the six parameters, estimation of CL, Q , V_c , and (V_p) require the pharmacokinetic data after the IV injection, estimation of k_a requires the pharmacokinetic data after the SC injection, and estimation of F requires the pharmacokinetic data after both IV and SC injections. In contrast, as the distribution phase contributes little to the pharmacokinetic profile, only three parameters (apparent CL [CL/F], apparent volume of distribution [V_d/F], and k_a) are needed to capture the pharmacokinetic profile of mAbs after SC injections. An approach that accurately predicts these three parameters in humans would be simpler than our previous approach. Moreover, if estimating the CL/F and V_d/F in humans only requires pharmacokinetic data from cynomolgus monkeys after a SC injection, then an IV injection becomes unnecessary, which improves animal welfare (3Rs, replacement, reduction, and refinement) and reduces costs.

In this study, we investigate multiple approaches for accurately predicting the pharmacokinetic parameters and profiles of mAbs after a SC injection in humans, and based on this analysis, we establish a simple and reliable approach using only three parameters (CL/F , V_d/F , and k_a).

2 Methods

2.1 Data Collection

First, to prepare the dataset for analysis, pharmacokinetic data of mAbs after SC injection in cynomolgus monkeys and humans were obtained from public sources (scientific articles, patents, and information provided by the Pharmaceutical and Medical Devices Agency and the US Food and Drug Administration). To eliminate the influence of target-mediated drug disposition, only mAbs showing linear pharmacokinetics in cynomolgus monkeys and humans were selected for analysis. The average values of pharmacokinetic parameters and plasma concentration–time profiles were collected from data sources. Plasma concentration–time profiles were obtained by scanning the figure from data sources using UnGraph 5 (Biosoft, Cambridge, United Kingdom). The concentration of mAbs in plasma was assumed to be the same in serum. If body weight information was not described in the data source, a body weight of 3 kg (cynomolgus monkey) and 75 kg (human) was used.

2.2 Prediction of Apparent Clearance and Apparent Volume of Distribution in Humans

In this study, to determine the best method for predicting CL/F and V_d/F of mAbs after a SC injection in humans, three approaches were investigated.

- Approach 1 Allometric scaling from CL/F and V_d/F in cynomolgus monkeys.
- Approach 2 Geometric mean of reported CL/F and V_d/F of 15 mAbs in humans.
- Approach 3 Prediction of V_d/F from predicted CL/F in humans using a linear regression analysis (derived equation is described in the results section) between CL/F and V_d/F (only for V_d/F).

2.3 Allometric Scaling

To determine the optimal scaling exponent of the allometric scaling approach for CL/F and V_d/F , the CL/F (mL/day) and V_d/F (mL) in humans were extrapolated from that in cynomolgus monkeys using the allometric scaling equation, with the scaling exponents of each parameter calculated using the following equations.

$$CL/F_{\text{human}} = CL/F_{\text{monkey}} \times \left(\frac{BW_{\text{human}}}{BW_{\text{monkey}}} \right)^{e_{CL/F}}$$

$$V_d/F_{\text{human}} = V_d/F_{\text{monkey}} \times \left(\frac{BW_{\text{human}}}{BW_{\text{monkey}}} \right)^{e_{V_d/F}}$$

BW and e represent body weight and scaling exponent, respectively. To estimate the optimal exponents for CL/F and V_d/F , the predictability of CL/F and V_d/F in humans was evaluated using several exponents.

2.4 Simulation of Plasma Concentration–Time Profiles of Monoclonal Antibodies after Subcutaneous Injections in Humans

To evaluate the applicability of this approach to the prediction of the plasma concentration–time profile of mAbs after SC injections in humans, the plasma concentration–time profile was simulated using a one-compartment model with first-order absorption and elimination as the following equations.

$$\frac{dA_a}{dt} = -k_a \times A_a$$

$$\frac{dA_c}{dt} = k_a \times A_a - k_{el} \times A_c$$

$$C_c = \frac{A_c}{V_d/F}$$

$$CL/F = k_{el} \times V_d/F$$

$$A_a(t = 0) = \text{Dose}$$

$$A_c(t = 0) = 0$$

$$C_c = \frac{k_a \times \text{Dose}}{(k_a \times V_d/F - CL/F)} \left\{ \exp\left(-\frac{CL/F}{V_d/F} \times t\right) - \exp(-k_a \times t) \right\}$$

A_a , A_c , k_{el} , and C_c represent the amount of mAb in the SC compartment, the amount in the central compartment, the elimination rate constant from the central compartment, and the concentration in the central compartment, respectively. Apparent CL predicted by approach 1 and V_d/F predicted by approach 3 and the geometric mean of k_a (0.287 (/day)) for mAbs after SC injections in humans were used in a simulation study. This study used the geometric mean of k_a (0.287 (/day)) calculated from data of total 19 mAbs in our previous report [12] as we previously found that k_a of mAbs after SC injections in humans showed small variability among mAbs. Furthermore, the geometric mean of k_a accurately predicted the plasma concentration–time profiles of mAbs after SC injections in humans in a previous study. Simulated plasma

concentration–time profiles of mAbs were compared with observed values.

2.5 Analysis

The simulation was conducted using SAAMII software (The Epsilon Group, Charlottesville, VA, USA). Linear regression analysis was performed using GraphPad Prism 6 (GraphPad Software, Inc., San Diego, CA, USA). The Pearson correlation coefficient r value was significant when $p < 0.05$. The parameters were compared using an unpaired t -test. The MAPE (mean absolute prediction error) was estimated to evaluate the prediction accuracy of CL/F and V_d/F in humans as follows:

$$\text{MAPE} = \frac{1}{n} \times \sum \sqrt{\left\{ \left(\frac{\text{Observed} - \text{Predicted}}{\text{Observed}} \right) \times 100 \right\}^2}$$

3 Results

3.1 Relationship between Pharmacokinetic Parameters

Fifteen mAbs were used for analysis. The pharmacokinetic parameters of mAbs after SC injections in cynomolgus monkeys and humans are listed in Table 1. The list consists of different IgG subclasses (IgG1 [11 mAbs], IgG2 [two mAbs], and IgG4 [two mAbs]) and mAbs against different target antigens. Figure 1 shows the distribution of CL/F and V_d/F in both species. The geometric mean of CL/F in cynomolgus monkeys and humans was 5.90 mL/day/kg (range 2.94–23.8) and 4.78 mL/day/kg (range 2.89–11.7), and V_d/F was 90.8 mL/kg (range 45.0–177) and 132 mL/kg (range 77.6–197), respectively. The geometric mean of CL/F in cynomolgus monkeys was slightly higher than in humans ($p = 0.27$). In contrast, the geometric mean of V_d/F was significantly lower in cynomolgus monkeys ($p = 0.0059$). Figure 2 shows the correlation of CL/F (A) and V_d/F (B) between cynomolgus monkeys and humans. While a significant correlation was observed for CL/F (Pearson $r = 0.782$, $p = 0.0006$), there was no clear correlation for V_d/F (Pearson $r = 0.345$, $p = 0.2083$). However, V_d/F and CL/F were significantly correlated with each other in humans (Pearson $r = 0.777$, $p = 0.0007$) (Fig. 2c). The equation of the linear regression line between CL/F (mL/day/kg) and V_d/F (mL/kg) in humans was as follows:

$$V_d/F_{\text{human}} (\text{mL/kg}) = 12.19 \times CL/F_{\text{human}} (\text{mL/day/kg}) + 73.46.$$

Table 1 Pharmacokinetic parameters of monoclonal antibodies after a subcutaneous injection in cynomolgus monkeys and humans

Antibody	Target	Subclass	Cynomolgus monkey		Human		References
			CL/F	V_d/F	CL/F	V_d/F	
			mL/day/kg	mL/kg	mL/day/kg	mL/kg	
DX-2930	Plasma kallikrein	IgG1	5.52	99.9	6.70	197	[27, 28]
CNT05825	IL-13	IgG1	6.90	80.6	3.55	143	[29, 30]
Mepolizumab/SB-240563	IL-5	IgG1	3.04	89.1	3.00	77.6	[31, 32]
Adalimumab	TNF α	IgG1	9.84	177	6.56	171	[33]
Omalizumab	IgE	IgG1	3.07	78.4	2.90	80.1	[34]
Golimumab	TNF α	IgG1	23.8	45.0	11.7	197	[35, 36]
Secukinumab	IL-17A	IgG1	2.94	79.3	2.89	98.6	[37]
ABT-981	IL-1 α and IL-1 β	IgG1	5.56	64.1	7.56	129	[38, 39]
Guselkumab	IL-23	IgG1	11.0	167	7.66	187	[40, 41]
Ustekinumab/CNT01275	IL-12/23	IgG1	3.79	75.4	3.10	97.3	[42, 43]
Risankizumab/ABBV-066	IL-23	IgG1	8.07	89.3	5.27	160	[44, 45]
Nemolizumab/CIM331	IL-31RA	IgG2	4.67	86.2	3.86	91.8	[46, 47]
AMG139	IL-23	IgG2	7.63	93.0	2.97	118	[48, 49]
ACE910	FIX and FX	IgG4	3.59	122	3.49	156	[50, 51]
Ixekizumab	IL-17A	IgG4	6.29	93.0	8.83	174	[52]
Geometric mean			5.90	90.8	4.78	132	

CL/F apparent clearance, IgE immunoglobulin E, IL interleukin, RA receptor A, TNF tumor necrosis factor, V_d/F apparent volume of distribution

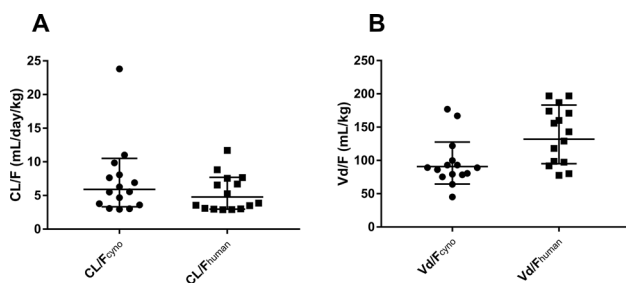


Fig. 1 Distribution of apparent clearance (CL/F) (a) and apparent volume of distribution (V_d/F) (b) of monoclonal antibodies in cynomolgus monkeys (closed circles) and humans (closed squares). Geometric means with 95% confidence intervals are shown. *cyno* cynomolgus monkeys

The Y -intercept of the regression line (73.46 (mL/kg)) was similar to reported V_d of mAbs [18]. This is reasonable because mAbs with small CL/F should show almost 100% F and small CL . Therefore, V_d/F should be close to V_d for mAbs with small CL/F .

3.2 Estimation of Optimal Exponent for Allometric Scaling

The optimal exponent of allometric scaling to predict CL/F and V_d/F of mAbs in humans from that in cynomolgus monkeys was investigated using data from 15 mAbs. Figure 3 shows the distribution of exponent for CL/F and V_d/F of 15

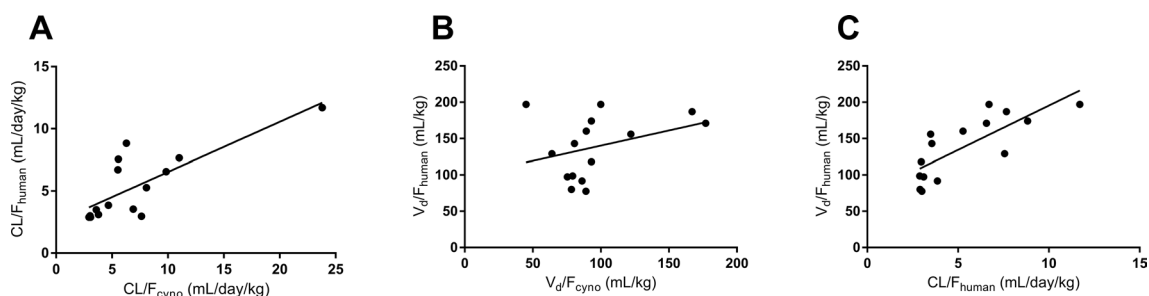


Fig. 2 Correlation of parameters between cynomolgus monkeys and humans. **a** Correlation of apparent clearance (CL/F) between cynomolgus monkeys and humans ($r=0.782$, $p=0.0006$). **b** Correlation

of apparent volume of distribution (V_d/F) between cynomolgus monkeys and humans ($r=0.345$, $p=0.2083$). **c** Correlation of CL/F and V_d/F in humans ($r=0.777$, $p=0.0007$). *cyno* cynomolgus monkeys

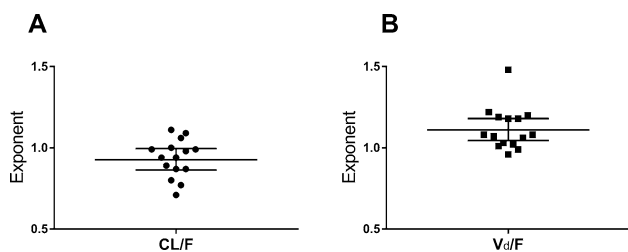


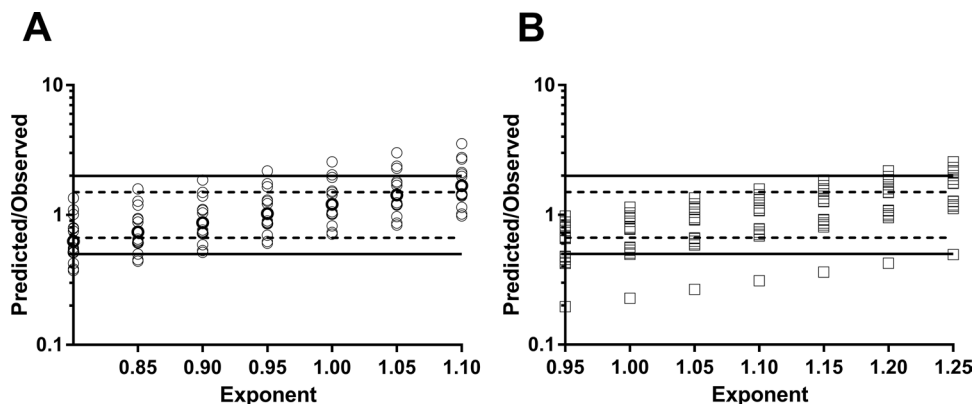
Fig. 3 Distribution of exponent for apparent clearance (CL/F) (a) and apparent volume of distribution (V_d/F) (b) of monoclonal antibodies. Geometric means with 95% confidence intervals are shown

mAbs. The geometric mean of exponent for CL/F and V_d/F was 0.93 and 1.11. In Fig. 4, the prediction accuracy of CL/F and V_d/F in humans was investigated using different exponents. The highest prediction accuracy was achieved with an exponent of 0.9 for CL/F and 1.1 for V_d/F . An exponent of 0.9 for CL/F showed 100% and 73% prediction accuracy within 2- and 1.5-fold of the observed value. An exponent of 1.1 for V_d/F showed 93% and 87% prediction accuracy within 2- and 1.5-fold of the observed value.

3.3 Comparison of Approaches to Predict Apparent Clearance and Apparent Volume of Distribution of Monoclonal Antibodies after Subcutaneous Injections in Humans

To select the best approach to predict CL/F and V_d/F of mAbs in humans, the prediction accuracy of three approaches were compared. In approach 1, an exponent of 0.9 for CL/F and 1.1 for V_d/F were used. For CL/F , this (MAPE = 30.9%) showed better prediction accuracy compared with approach 2 (MAPE = 43.0%). As shown earlier, approach 1, using an exponent of 0.9 for CL/F , showed 100% and 73% prediction accuracy within 2- and 1.5-fold of the observed value. However, for V_d/F , approach 3 (MAPE = 18.9%) was the best among three approaches

Fig. 4 Prediction accuracy of apparent clearance (a) and apparent volume of distribution (b) of monoclonal antibodies in humans using different exponents. Solid and dashed lines indicate 2.0- and 1.5-fold difference from the observed value



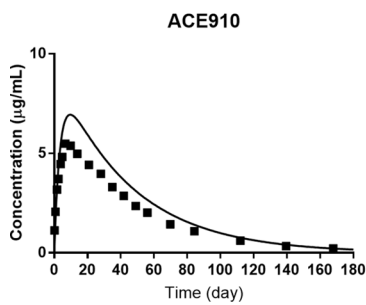
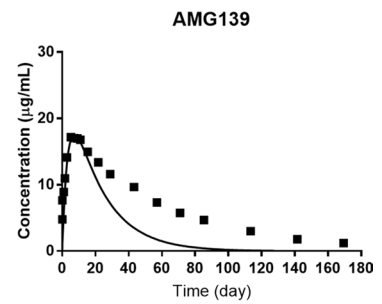
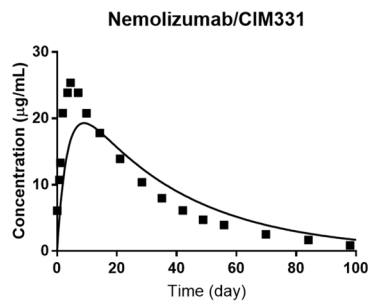
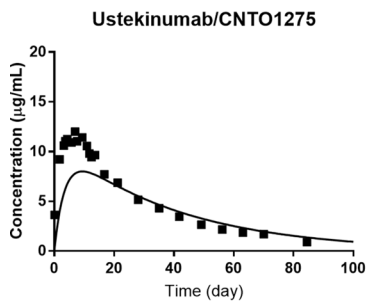
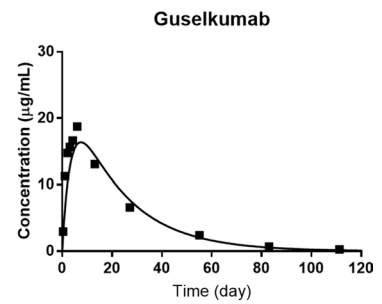
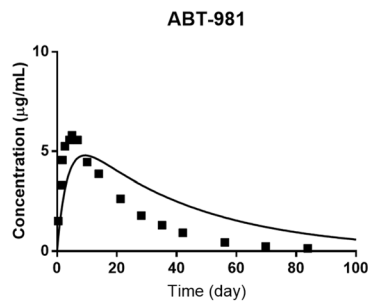
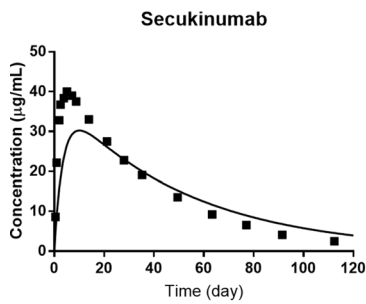
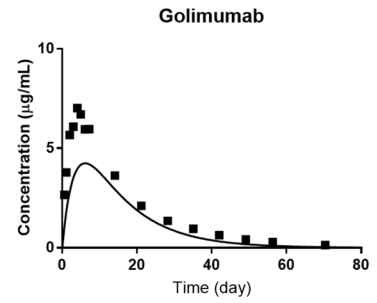
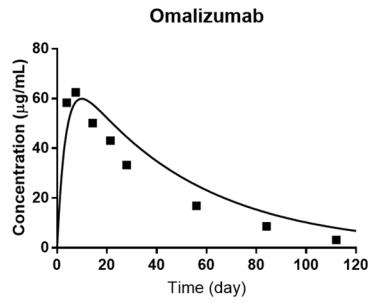
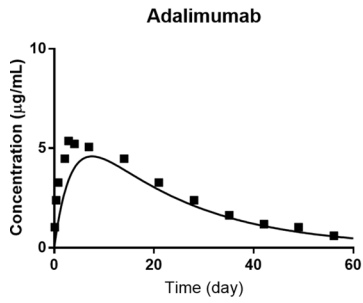
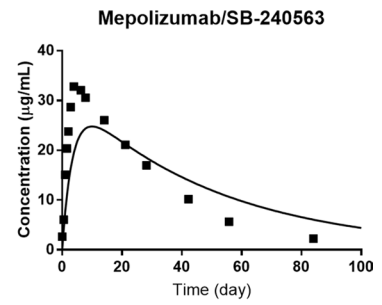
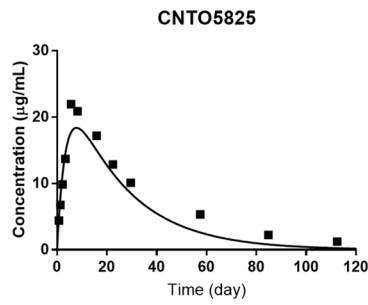
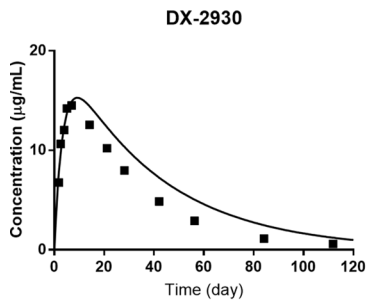
(MAPE = 28.5% for approach 1, MAPE = 29.7% for approach 2). Approach 3 for V_d/F showed 100% prediction accuracy within 1.5-fold of the observed value. The combination of approach 1 for CL/F and approach 3 for V_d/F was selected to predict the plasma concentration–time profile of mAbs after SC injections in humans.

3.4 Prediction of Plasma Concentration–Time Profile of Monoclonal Antibodies after Subcutaneous Injection in Humans

The CL/F from approach 1 (allometric scaling), V_d/F from approach 3 (linear regression), and the geometric mean of k_a (0.287 /day) was used to predict the plasma concentration–time profiles of 13 mAbs after SC injections in humans. Risankizumab and ixekizumab were removed from the data set because the appropriate plasma concentration–time profiles for those mAbs were not available. Figure 5 shows the observed and predicted plasma concentration–time profiles of 13 mAbs after SC injections in humans. Figure 6 shows the overall relationship between observed and predicted values. As shown in Fig. 5, the elimination phase of only AMG139 was clearly under-predicted by this approach.

4 Discussion

In this study, we investigated a simple approach for predicting the pharmacokinetic profiles of mAbs after SC injections in humans using only three parameters (CL/F , V_d/F , and k_a). As described earlier, we previously proposed an approach that used six parameters and required pharmacokinetic data after IV injections in cynomolgus monkeys. However, data after SC injections in cynomolgus monkeys are required to expect the exposure of mAbs after SC injections in a toxicology study when that delivery route is intended for a clinical trial. Thus, to simplify the process and reduce the amount of required data, we proposed a new approach to predict the pharmacokinetics of mAbs after SC injections in humans.



◀**Fig. 5** Predicted and observed plasma concentration–time profiles of monoclonal antibodies after a subcutaneous injection in humans. Closed squares indicate observed average plasma concentrations of monoclonal antibodies. Solid lines indicate predicted plasma concentration–time profiles of monoclonal antibodies

In this study, we observed a significant positive correlation between the CL/F of mAbs in cynomolgus monkeys and humans. This is a first report of such a correlation. We and other groups have reported that CL of mAbs in humans can be accurately predicted from that in cynomolgus monkeys using allometric scaling [12, 18, 19]. We also reported a significant correlation between CL after an IV injection and F after a SC injection in humans, which indicated that mAbs with higher CL show lower F after a SC injection. Therefore, the significant positive correlation of CL/F after a SC injection between cynomolgus monkeys and humans is considered to be reasonable. Because of the significant positive correlation of CL/F between cynomolgus monkeys and humans, the allometric scaling approach (approach 1) was able to reliably predict CL/F in humans. We [12], Deng et al. [19], and Dong et al. [20] reported that the allometric scaling of data from cynomolgus monkeys showed 71% (17 out of 24 mAbs), 85% (11 out of 13 mAbs), and 50% (5 out of 10 mAbs) predictability of CL after an IV injection in humans within 1.5-fold of the observed value. Approach 1 for CL/F showed comparable accuracy (100% and 73% prediction accuracy within 2- and 1.5-fold of the observed value) with a previous report for CL . We estimated that 0.9 was the best exponent for predicting CL/F with this approach. However, we [12], Deng et al. [19], and Dong et al. [20] proposed using 0.8, 0.85, and 0.75 as exponents to predict CL in humans from that in cynomolgus monkeys using the allometric scaling approach. The optimal exponents for CL and CL/F are different because of F . It has been reported that F of mAbs after a SC injection in humans tended to be lower than that in cynomolgus monkeys [21]. Thus, the optimal exponent of CL/F would be slightly higher than that of CL .

In this analysis, the elimination phase of AMG139 was under-predicted. Our previous study also showed this under-prediction for AMG139 after an IV injection in humans using the allometric scaling approach from cynomolgus monkeys [12]. This was because of the lower than expected CL of AMG139 in humans based on CL in cynomolgus monkeys. Therefore, the under-prediction for AMG139 is probably owing to the poor translationality of CL between cynomolgus monkeys and humans. As AMG139 is an IgG2-based anti-interleukin-23 monoclonal antibody, there has been reported to be no atypical characteristics of AMG139 compared to other mAbs. Because the exact reason for the under-prediction of AMG139 is still unknown, it remains an issue for the prediction of pharmacokinetics of mAbs in humans.

In contrast, there was no significant correlation in V_d/F between cynomolgus monkeys and humans. Thus, approach 1 (allometric scaling) showed a similar MAPE with approach 2 (geometric mean). Moreover, in this study, we found a significant correlation between V_d/F and CL/F in humans. Several previous reports showed no significant correlation between CL and V_d in humans [18, 20]. Therefore, as both CL/F and V_d/F have the same F as a denominator, it is reasonable that a positive correlation was observed between CL/F and V_d/F in humans. Furthermore, as described above, we previously reported a correlation between CL after an IV injection and F after a SC injection in humans [12]. This correlation between CL and F makes the correlation between CL/F and V_d/F clearer. Because of the significant correlation between CL/F and V_d/F in humans, approach 3 showed the lowest MAPE. Dong et al. [20] reported that the allometric scaling approach of data from cynomolgus monkeys showed 50% (five out of ten mAbs) predictability for V_d after an IV injection in humans within 1.5-fold of the observed value. Approach 3 showed superior accuracy (100% prediction accuracy within 1.5-fold of the observed value) for V_d/F than a previous report for V_d .

In this study, only mAbs with linear pharmacokinetics were used for analysis. Generally, non-linear pharmacokinetics of mAbs is analyzed by a Michaelis–Menten model or the target-mediated drug disposition model [22, 23]. These models separately provide linear (CL , Q , V_c , V_p or CL/F , V_d/F) and non-linear (Michaelis–Menten constant, maximum elimination rate, or internalization rate constant, total target concentration, target elimination rate constant, target production rate constant) pharmacokinetic parameters [24]. Even for mAbs with non-linear pharmacokinetics, linear pharmacokinetic parameters are needed to capture the plasma concentration–time profiles. Therefore, this approach should also be valuable to predict linear pharmacokinetic parameters after a SC injection of mAbs, which show non-linear pharmacokinetics in humans. This point should be investigated in the future.

For prediction of pharmacokinetics of mAbs after a SC injection in humans, use of mini-pigs and in vitro tools has been reported. Zheng et al. [25] reported that F of mAbs after a SC injection in humans was weakly correlated with that in mini-pigs. While a mini-pig study can estimate a slight tendency of F in humans, mAbs often failed to show cross-reactivity against the target antigen in the mini-pigs, making them unsuitable for the types of efficacy/toxicology studies required for preclinical development. Thus, cynomolgus monkey studies continue to be necessary. Additionally, our proposed method appears to achieve greater prediction accuracy than the mini-pig-based estimations. Furthermore, Bown et al. [26] reported that an in vitro tool, termed Scissor, accurately predicted F of mAbs after a SC injection in

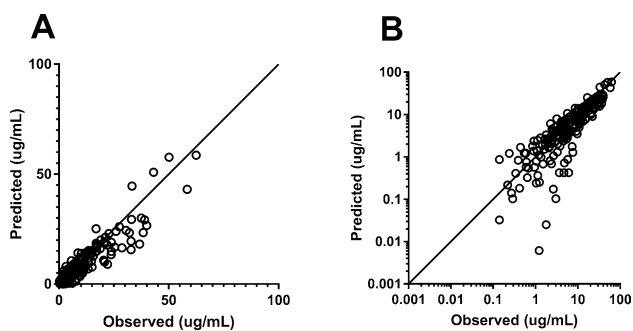


Fig. 6 Goodness-of-fit plot of observed and predicted plasma concentrations of monoclonal antibodies after a subcutaneous injection in humans (**a**, normal scale; **b**, log scale). Open circles indicate observed and predicted plasma concentrations of monoclonal antibodies. Solid line indicates 100% prediction line

humans. Scissor mimics the physiological conditions in the SC environment using an extracellular matrix and optimal buffer. Although the study used only eight mAbs to evaluate the predictability of F , the combination of an animal study and in vitro assay can be an important strategy to improve animal welfare in the future.

5 Conclusions

We established a new approach that accurately predicts the pharmacokinetic profile of mAbs after a SC injection in humans using only three parameters (CL/F , V_d/F , and k_a). This approach consists of only three steps.

First step	Prediction of CL/F in humans from that in cynomolgus monkeys using allometric scaling with a fixed exponent of 0.9.
Second step	Prediction of V_d/F in humans from predicted CL/F in humans using a linear regression equation.
Third step	Simulation of the plasma concentration–time profile of mAbs after a SC injection in humans using predicted CL/F and V_d/F and the geometric mean of k_a (0.287 (/day)) in humans.

This approach does not require pharmacokinetic data after an IV injection in cynomolgus monkeys. Thus, this approach can improve animal welfare and reduce costs in the development of mAbs.

Compliance with Ethical Standards

Funding This work was fully supported by Chugai Pharmaceutical Co. Ltd.

Conflict of interest Kenta Haraya and Tatsuhiko Tachibana are employees of Chugai Pharmaceutical Co. Ltd. and declare no potential conflicts of interest that might be relevant to the content of this article.

Ethics approval Not applicable.

Consent to participate Not applicable.

Consent for publication Not applicable.

Availability of data and material All pharmacokinetic data is available in reference and all software is commercially available.

Code availability Not applicable.

Authors' contributions K.H. and T.T. contributed to the study concept, data analysis and preparation of manuscript.

References

1. Tsumoto K, Isozaki Y, Yagami H, Tomita M. Future perspectives of therapeutic monoclonal antibodies. *Immunotherapy*. 2019;11(2):119–27. <https://doi.org/10.2217/imt-2018-0130>.
2. Ecker DM, Jones SD, Levine HL. The therapeutic monoclonal antibody market. *mAbs*. 2015;7(1):9–14. <https://doi.org/10.4161/19420862.2015.989042>.
3. Ryman JT, Meibohm B. Pharmacokinetics of monoclonal antibodies. *CPT Pharmacometrics Syst Pharmacol*. 2017;6(9):576–88. <https://doi.org/10.1002/psp4.12224>.
4. Viola M, Sequeira J, Seica R, Veiga F, Serra J, Santos AC, et al. Subcutaneous delivery of monoclonal antibodies: how do we get there? *J Control Release*. 2018;286:301–14. <https://doi.org/10.1016/j.jconrel.2018.08.001>.
5. Igawa T, Ishii S, Tachibana T, Maeda A, Higuchi Y, Shimaoka S, et al. Antibody recycling by engineered pH-dependent antigen binding improves the duration of antigen neutralization. *Nat Biotechnol*. 2010;28(11):1203–7. <https://doi.org/10.1038/nbt.1691>.
6. Igawa T, Maeda A, Haraya K, Tachibana T, Iwayanagi Y, Mimoto F, et al. Engineered monoclonal antibody with novel antigen-sweeping activity in vivo. *PLoS ONE*. 2013;8(5):e63236. <https://doi.org/10.1371/journal.pone.0063236>.
7. Haraya K, Tachibana T, Iwayanagi Y, Maeda A, Ozeki K, Nezu J, et al. PK/PD analysis of a novel pH-dependent antigen-binding antibody using a dynamic antibody-antigen binding model. *Drug Metab Pharmacokinet*. 2016;31(2):123–32. <https://doi.org/10.1016/j.dmpk.2015.12.007>.
8. Igawa T, Haraya K, Hattori K. Sweeping antibody as a novel therapeutic antibody modality capable of eliminating soluble antigens from circulation. *Immunol Rev*. 2016;270(1):132–51. <https://doi.org/10.1111/imr.12392>.
9. Shpilberg O, Jackisch C. Subcutaneous administration of rituximab (MabThera) and trastuzumab (Herceptin) using hyaluronidase. *Br J Cancer*. 2013;109(6):1556–611. <https://doi.org/10.1038/bjc.2013.371>.
10. Haraya K, Tachibana T, Igawa T. Improvement of pharmacokinetic properties of therapeutic antibodies by antibody engineering. *Drug Metab Pharmacokinet*. 2019;34(1):25–41. <https://doi.org/10.1016/j.dmpk.2018.10.003>.
11. Iwasaki K, Uno Y, Utoh M, Yamazaki H. Importance of cynomolgus monkeys in development of monoclonal antibody drugs. *Drug Metab Pharmacokinet*. 2019;34(1):55–63. <https://doi.org/10.1016/j.dmpk.2018.02.003>.

12. Haraya K, Tachibana T, Nezu J. Quantitative prediction of therapeutic antibody pharmacokinetics after intravenous and subcutaneous injection in human. *Drug Metab Pharmacokinet.* 2017;32(4):208–17. <https://doi.org/10.1016/j.dmpk.2017.05.002>.
13. Oitate M, Nakayama S, Ito T, Kurihara A, Okudaira N, Izumi T. Prediction of human plasma concentration-time profiles of monoclonal antibodies from monkey data by a species-invariant time method. *Drug Metab Pharmacokinet.* 2012;27(3):354–9. <https://doi.org/10.2133/dmpk.dmpk-11-sh-059>.
14. Nnane IP, Han C, Jiao Q, Tam SH, Davis HM, Xu Z. Modification of the Fc region of a human anti-oncostatin M monoclonal antibody for higher affinity to FcRn receptor and extension of half-life in cynomolgus monkeys. *Basic Clin Pharmacol Toxicol.* 2017;121(1):13–211. <https://doi.org/10.1111/bcpt.12761>.
15. Haraya K, Tachibana T, Nezu J. Predicting pharmacokinetic profile of therapeutic antibodies after iv injection from only the data after sc injection in cynomolgus monkey. *Xenobiotica.* 2017;47(3):194–201. <https://doi.org/10.1080/00498254.2016.1174792>.
16. Oh CK, Faggioni R, Jin F, Roskos LK, Wang B, Birrell C, et al. An open-label, single-dose bioavailability study of the pharmacokinetics of CAT-354 after subcutaneous and intravenous administration in healthy males. *Br J Clin Pharmacol.* 2010;69(6):645–55. <https://doi.org/10.1111/j.1365-2125.2010.03647.x>.
17. Struemper H, Thapar M, Roth D. Population pharmacokinetic and pharmacodynamic analysis of belimumab administered subcutaneously in healthy volunteers and patients with systemic lupus erythematosus. *Clin Pharmacokinet.* 2018;57(6):717–28. <https://doi.org/10.1007/s40262-017-0586-5>.
18. Oitate M, Masubuchi N, Ito T, Yabe Y, Karibe T, Aoki T, et al. Prediction of human pharmacokinetics of therapeutic monoclonal antibodies from simple allometry of monkey data. *Drug Metabol Pharmacokinet.* 2011;26(4):423–30.
19. Deng R, Iyer S, Theil FP, Mortensen DL, Fielder PJ, Prabhu S. Projecting human pharmacokinetics of therapeutic antibodies from nonclinical data: what have we learned. *mAbs.* 2011;3(1):61–6. <https://doi.org/10.4161/mabs.3.1.13799>.
20. Dong JQ, Salinger DH, Endres CJ, Gibbs JP, Hsu CP, Stouch BJ, et al. Quantitative prediction of human pharmacokinetics for monoclonal antibodies: retrospective analysis of monkey as a single species for first-in-human prediction. *Clin Pharmacokinet.* 2011;50(2):131–42. <https://doi.org/10.2165/11537430-000000000-00000>.
21. Richter WF, Bhansali SG, Morris ME. Mechanistic determinants of biotherapeutics absorption following SC administration. *AAPS J.* 2012;14(3):559–70. <https://doi.org/10.1208/s12248-012-9367-0>.
22. Luu KT, Bergqvist S, Chen E, Hu-Lowe D, Kraynov E. A model-based approach to predicting the human pharmacokinetics of a monoclonal antibody exhibiting target-mediated drug disposition. *J Pharmacol Exp Ther.* 2012;341(3):702–8. <https://doi.org/10.1124/jpet.112.191999>.
23. Wiczling P, Rosenzweig M, Vaickus L, Jusko WJ. Pharmacokinetics and pharmacodynamics of a chimeric/humanized anti-CD3 monoclonal antibody, oteelixumab (TRX4), in subjects with psoriasis and with type 1 diabetes mellitus. *J Clin Pharmacol.* 2010;50(5):494–506. <https://doi.org/10.1177/0091270009349376>.
24. Yan X, Mager DE, Krzyzanski W. Selection between Michaelis-Menten and target-mediated drug disposition pharmacokinetic models. *J Pharmacokinet Pharmacodyn.* 2010;37(1):25–47. <https://doi.org/10.1007/s10928-009-9142-8>.
25. Zheng Y, Tesar DB, Benincosa L, Birnbock H, Boswell CA, Bumbaca D, et al. Minipig as a potential translatable model for monoclonal antibody pharmacokinetics after intravenous and subcutaneous administration. *mAbs.* 2012;4(2):243–55. <https://doi.org/10.4161/mabs.4.2.19387>.
26. Bown HK, Bonn C, Yohe S, Yadav DB, Patapoff TW, Daugherty A, et al. In vitro model for predicting bioavailability of subcutaneously injected monoclonal antibodies. *J Controlled Release.* 2018;273:13–20. <https://doi.org/10.1016/j.jconrel.2018.01.015>.
27. Kenniston JA, Faucette RR, Martik D, Comeau SR, Lindberg AP, Kopacz KJ, et al. Inhibition of plasma kallikrein by a highly specific active site blocking antibody. *J Biol Chem.* 2014;289(34):23596–608. <https://doi.org/10.1074/jbc.M114.569061>.
28. Chyung Y, Vince B, Iarrobino R, Sexton D, Kenniston J, Faucette R, et al. A phase 1 study investigating DX-2930 in healthy subjects. *Ann Allergy Asthma Immunol.* 2014;113(4):460–6. <https://doi.org/10.1016/j.anaai.2014.05.028>.
29. Nnane IP, Xu Z, Zhou H, Davis HM. Non-clinical pharmacokinetics, prediction of human pharmacokinetics and first-in-human dose selection for CNTO 5825, an anti-interleukin-13 monoclonal antibody. *Basic Clin Pharmacol Toxicol.* 2015;117(4):219–25. <https://doi.org/10.1111/bcpt.12391>.
30. van Hartingsveldt B, Nnane IP, Bouman-Thio E, Loza MJ, Piantone A, Davis HM, et al. Safety, tolerability and pharmacokinetics of a human anti-interleukin-13 monoclonal antibody (CNTO 5825) in an ascending single-dose first-in-human study. *Br J Clin Pharmacol.* 2013;75(5):1289–98. <https://doi.org/10.1111/j.1365-2125.2012.04477.x>.
31. Zia-Amirhosseini P, Minthorn E, Benincosa LJ, Hart TK, Hottenstein CS, Tobia LA, et al. Pharmacokinetics and pharmacodynamics of SB-240563, a humanized monoclonal antibody directed to human interleukin-5, in monkeys. *J Pharmacol Exp Ther.* 1999;291(3):1060–7.
32. Smith DA, Minthorn EA, Beerahee M. Pharmacokinetics and pharmacodynamics of mepolizumab, an anti-interleukin-5 monoclonal antibody. *Clin Pharmacokinet.* 2011;50(4):215–27. <https://doi.org/10.2165/11584340-000000000-00000>.
33. PMDA. Adalimumab (Humira). 2008. <https://www.pmda.go.jp/drugs/2008/P200800019/index.html>. Accessed 1 Nov 2019.
34. PMDA. Omalizumab (Xolair). 2013. <https://www.pmda.go.jp/drugs/2013/P201300105/index.html>. Accessed 1 Nov 2019.
35. PMDA. Golimumab (Simponi). 2011. <https://www.pmda.go.jp/drugs/2011/P201100114/index.html>. Accessed 1 Nov 2019.
36. Zhuang Y, Lyn S, Lv Y, Xu Z, Bouman-Thio E, Masterson T, et al. Pharmacokinetics and safety of golimumab in healthy Chinese subjects following a single subcutaneous administration in a randomized phase I trial. *Clin Drug Invest.* 2013;33(11):795–800. <https://doi.org/10.1007/s40261-013-0124-7>.
37. PMDA. Secukinumab (Cosentyx). 2014. <https://www.pmda.go.jp/drugs/2014/P201400171/index.html>. Accessed 1 Nov 2019.
38. Lacy SE, Wu C, Ambrosi DJ, Hsieh CM, Bose S, Miller R, et al. Generation and characterization of ABT-981, a dual variable domain immunoglobulin (DVD-Ig(TM)) molecule that specifically and potently neutralizes both IL-1alpha and IL-1beta. *mAbs.* 2015;7(3):605–19. <https://doi.org/10.1080/19420862.2015.1026501>.
39. Kosloski MP, Goss S, Wang SX, Liu J, Loebbert R, Medema JK, et al. Pharmacokinetics and tolerability of a dual variable domain immunoglobulin ABT-981 against IL-1alpha and IL-1beta in healthy subjects and patients with osteoarthritis of the knee. *J Clin Pharmacol.* 2016;56(12):1582–90. <https://doi.org/10.1002/jcp.764>.
40. US FDA. Guselkumab (Tremfya). 2016. https://www.accessdata.fda.gov/drugsatfda_docs/nda/2017/761061Orig1s000MultidisciplineR.pdf. Accessed 1 Nov 2019.
41. Zhuang Y, Calderon C, Marciniak SJ Jr, Bouman-Thio E, Szapary P, Yang TY, et al. First-in-human study to assess guselkumab (anti-IL-23 mAb) pharmacokinetics/safety in healthy subjects and patients with moderate-to-severe psoriasis. *Eur J Clin*

- Pharmacol. 2016;72(11):1303–10. <https://doi.org/10.1007/s00228-016-2110-5>.
42. PMDA. Ustekinumab (Stelara). 2011. <https://www.pmda.go.jp/drugs/2011/P201100021/index.html>. Accessed 1 Nov 2019.
 43. Zhu Y, Wang Q, Frederick B, Bouman-Thio E, Marini JC, Keen M, et al. Comparison of the pharmacokinetics of subcutaneous ustekinumab between Chinese and non-Chinese healthy male subjects across two phase 1 studies. *Clin Drug Invest.* 2013;33(4):291–301. <https://doi.org/10.1007/s40261-013-0072-2>.
 44. PMDA. Risankizumab (Skyrizi). 2019. https://www.pmda.go.jp/drugs/2019/P20190329001/112130000_23100AMX00299_A100_1.pdf. Accessed 1 Nov 2019.
 45. Suleiman AA, Khatri A, Minocha M, Othman AA. Population pharmacokinetics of the interleukin-23 inhibitor risankizumab in subjects with psoriasis and Crohn's disease: analyses of phase I and II trials. *Clin Pharmacokinet.* 2019;58(3):375–87. <https://doi.org/10.1007/s40262-018-0704-z>.
 46. Oyama S, Kitamura H, Kuramochi T, Higuchi Y, Matsushita H, Suzuki T, et al. Cynomolgus monkey model of interleukin-31-induced scratching depicts blockade of human interleukin-31 receptor A by a humanized monoclonal antibody. *Exp Dermatol.* 2018;27(1):14–211. <https://doi.org/10.1111/exd.13236>.
 47. Nemoto O, Furue M, Nakagawa H, Shiramoto M, Hanada R, Matsuki S, et al. The first trial of CIM331, a humanized antihuman interleukin-31 receptor A antibody, in healthy volunteers and patients with atopic dermatitis to evaluate safety, tolerability and pharmacokinetics of a single dose in a randomized, double-blind, placebo-controlled study. *Br J Dermatol.* 2016;174(2):296–304. <https://doi.org/10.1111/bjd.14207>.
 48. Kock K, Pan WJ, Gow JM, Horner MJ, Gibbs JP, Colbert A, et al. Preclinical development of AMG 139, a human antibody specifically targeting IL-23. *Br J Pharmacol.* 2015;172(1):159–72. <https://doi.org/10.1111/bph.12904>.
 49. Gibbs JP, Tsuji W, PAN WJ. Methods for treating psoriasis using an anti-IL-23 antibody. Patent (WO2014149425). 2014.
 50. Muto A, Yoshihashi K, Takeda M, Kitazawa T, Soeda T, Igawa T, et al. Anti-factor IXa/X bispecific antibody (ACE910): hemostatic potency against ongoing bleeds in a hemophilia A model and the possibility of routine supplementation. *J Thromb Haemost.* 2014;12(2):206–13.
 51. Uchida N, Sambe T, Yoneyama K, Fukazawa N, Kawanishi T, Kobayashi S, et al. A first-in-human phase I study of ACE910, a novel factor VIII-mimetic bispecific antibody, in healthy subjects. *Blood.* 2016;127(13):1633–41. <https://doi.org/10.1182/blood-2015-06-650226>.
 52. PMDA. Ixekizumab (Taltz). 2016. <https://www.pmda.go.jp/drugs/2016/P20160725001/index.html>. Accessed 1 Nov 2019.